

Characterization of Polymeric Coatings

Subjects: Materials Science, Coatings & Films | Polymer Science | Electrochemistry

Contributor: Andressa Trentin, Amirhossein Pakseresht, Alicia Duran, Yolanda Castro, Dušan Galusek

The development of anti-corrosion polymeric coatings has grown exponentially in the fields of material science, chemistry, engineering, and nanotechnology and has prompted the evolution of efficient characterization techniques. Polymeric coatings represent a well-established protection system that provides a barrier between a metallic substrate and the environment. However, the increase in complexity and functionality of these coatings requires high-precision techniques capable of predicting failures and providing smart protection.

Keywords: polymeric coatings ; anti-corrosion ; corrosion inhibitor

1. Accelerated Corrosion Tests

Accelerated corrosion tests are employed by engineers and materials scientists to speed up the degradation process and to understand the reactions that occur in metals coated with polymeric coatings ^{[1][2]}. The main practices include the salt-spray test (continuous salt fog) and cyclic corrosion test, also known as Prohesion test (wet-dry intervals) ^[3]. Although the lack of correlation to field studies has been the subject of debate, specifications such as those of the American Society for Testing and Materials (ASTM) have been adapted accordingly and are widely employed by laboratories and industries ^[1].

1.1. Salt-Spray Tests

Salt spray, also known as the salt fog test, consists of uninterrupted exposure of intact or damaged coated substrates to a salty fog solution (5% sodium chloride) in a chamber. Parameters such as temperature, pH, air pressure, duration of the test and UV radiation are usually pre-determined by the operator ^[3]. The salt-spray test has undergone several modifications so that laboratory assays are comparable with field tests, usually carried out over 5 years ^[2]. One of the main advantages includes its relatively inexpensive and easy procedure that provides quick comparative results. One must take into account, however, that this qualitative analysis does not represent real-world conditions and besides destructive, it provides results for saline environments only.

It is known that ultraviolet (UV) radiation, humidity, temperature, pH, and the presence of oxygen and salt are the main driving forces that contribute to the onset of corrosion and the failure of films ^{[4][5]}. Factors that affect the reproducibility of results, such as the effects of pH, fog sedimentation rate, air pressure, temperature, sample position, solution concentration and so on, were established after extensive research and are currently used by the suppliers of these devices ^[2]. The evolution of ASTM specifications to the current B117 has provided the necessary practices to develop salt-spray chambers and accessories that allow for the control of accelerated corrosion tests ^[5]. For this purpose, some conditions must be fulfilled, namely (i) the same corrosion mechanism as in real-world conditions, (ii) the relationship between measured and varied parameters, and (iii) the same probability of the results distribution ^[6].

Salt-spray tests are particularly useful for investigating the mechanism of action for corrosion inhibitors loaded into intact or scribed coatings. Interesting results were found by comparing the activity of inhibitors based on chromates, lithium, and other chromate-free substances ^[2].

Duong et al. performed a salt-spray one of hydrotalcite-containing epoxy coatings modified with 2-benzothiazolythio-succinic acid (B TSA) and benzoate (BZ) as the inhibitors. The results reveal the potential of corrosion inhibition when 1.5% BZ is added to the material ^[8]. The evaluation of the coatings after 96 h of salt-spray exposure shows a lower degree of delamination and formation of corrosion products when the inhibitor is present compared to the unmodified epoxy coating. It was attributed that this effect to the low solubility of the benzoate in water and the more intense leaching in the scratched area, limiting the spread of corrosion ^[8]. Other examples of accelerated corrosion tests applied to self-healing coatings include immersion in 3.5 wt.% NaCl solution (NACE/ASTM TMO169/G31) for 75 days ^[9], the Q-panel condensation (QCT) test performed at 41° C, continuous condensation without drying (ASTM D 4585-99) for 1000 h ^[10], or the Prohesion cyclic test for 4896 h (ASTM G85-09) ^[11].

2. Conventional Electrochemical Analysis

Electrochemical tests are the state of the art in the evaluation of anti-corrosion coatings. The conventional methods are considered efficient tools to monitor the degradation of an average of the electrochemical processes taking place on the surface of the working electrode. Some of the main practices in coatings evaluation consist of open-circuit potential (OCP) and electrochemical impedance spectroscopy (EIS). Other common tests include linear polarization resistance (LPR), electrochemical noise (EN), electrochemical frequency modulation (EFM), potentiostatic step polarization, and galvanostatic step polarization [12]. Nonetheless, the next sections describe the principles, examples, advantages, and limitations of OCP and EIS.

2.1. Open-Circuit Potential (OCP)

The open-circuit potential is the potential of a working electrode when no current is applied to the cell [13]. Tracking the OCP is a useful practice for monitoring the degradation of barrier coatings since the passage of electrons through the coating causes the OCP value to drop to the metal substrate [13]. It is known that more negative potentials in time-potential measurements may indicate the removal of oxide layers from the surface and initiation of corrosion, while more positive potentials indicate the beginning of a protective film formation. However, the corrosion potential itself can be an erroneous indicator of corrosion as nobler potentials do not necessarily suggest slower corrosion rates [14]. This was explained by the pioneering work of Evans and later by Pourbaix using potential-pH diagrams, where a positive shift of pH within an active corrosion zone increases the corrosion rate, not the opposite [14][15]. In conclusion, electrochemical measurements correlated to the results of accelerated corrosion tests are found to be more reliable and reproducible.

In potentiometry, the potential of an electrode is measured in relation to another standardized electrode. This is known as the open-circuit potential or corrosion potential (OCP or E_{OC}) [13]. OCP measurements are typically employed before EIS measurements to verify the system's stability. The main advantages of the technique rely on its simple setup that provides the user with a semi-quantitative evaluation of coatings which can be associated with electrochemical impedance spectroscopy results. Although their values do not provide a direct estimate of corrosion protection, some were reported a direct correlation with low-frequency modulus values of electrochemical impedance measurements ($|Z|_{lf}$) [16] or pore resistance (R_{po}) values [17]. The repassivation cycles of substrates by conducting coatings containing corrosion inhibitors can be easily identified by OCP [18].

2.2. Electrochemical Impedance Spectroscopy (EIS)

The possibility of estimating the performance of barrier coatings, water uptake/polymeric swelling, presence of defects, interface reactivity, adhesion, and the assessment of parameters such as the coating delamination index, coating damage index, low-frequency impedance, breakpoint frequency, and high-frequency phase angle has made EIS one of the most powerful tools for evaluating the performance of coatings [19][20][21][22]. Overall, EIS is an extremely useful technique to measure and monitor the rate of deterioration of polymeric coatings exposed to electrolytes and to study electrochemical cathodic and anodic reactions when corrosion occurs. Some of the main advantages of EIS of polymeric coatings include, but are not limited to, a non-destructive nature, assessment of the degradation or regeneration of films, and most importantly, providing quantitative values for the electrochemical processes taking place in the system [23]. Nonetheless, the results correspond to an average of the surface, and modeling and interpreting diffusing or corroding systems can be complex.

To obtain quantitative information on the electrochemical processes taking place at the coating–oxide–metal interface it is common to combine resistors and capacitors to represent the behavior of the material in the form of an electrical equivalent circuit. The resistance can represent the electron transfer reactions that occur during corrosion [20]. However, the concept of resistance introduced by Ohm's law ($R = V/I$, where R is the resistance in ohms, V is the voltage in volts, and I is the current in amperes) is limited only to the resistor and it does not apply to complex, real-world systems. To contour this problem, the impedance formalism (Z) is applied. Z is the tendency of a circuit to resist the flow of an alternating electric current [23] and is mathematically represented by the expression $Z = V_{ac}/I_{ac}$. Typically, a sinusoidal voltage disturbance is applied to the system in the range of ± 10 mV, resulting in sinusoidal current waves with a phase shift between them, known as ϕ . The impedance is mostly represented either in the Nyquist format ($Z_{imaginary}$ vs. Z_{real}) as Bode plots ($|Z|$ vs. frequency (f)) and/or as a phase angle plot (ϕ vs. f) [19][20][21].

As the coating deteriorates with the uptake of water and ions, the film presents more resistive features. These features are identified by more stable values of the open-circuit potential and by a decrease in the impedance modulus and phase angle values at low frequencies ($f < 1$ Hz) [20].

When in contact with a solution under an alternating voltage, a good coating can be described as a capacitor (a non-conductive physical barrier between metal and electrolyte) [13][24]. High-performance coatings usually exhibit highly capacitive behavior in the early stages of immersion, acting almost as an ideal capacitor. This behavior depends on the thickness and dielectric constant values of the coating [20]. Nevertheless, electrolyte absorption leads to an uneven distribution of electrical properties, resulting in deviations from simple capacitive behavior. Taking into account the non-ideality of the system, a constant phase element (CPE) is normally used during modeling by electrical equivalent circuits (EEC) to replace the capacitor, providing a good correlation with experimental data [25]. The changes in the coating structure caused by the swelling of the polymeric chains are reflected in the physical properties of the material and, consequently, in the EECs that best describe the behavior of the immersed coating. Depending on the reactions taking place in the film, the circuits used to describe the systems can vary (**Figure 1**).

In the case of short-time immersion in an electrolyte, the properties of a barrier coating remain intact. In this period, the electrolyte resistance (R_s), the capacitance or CPE (CPE_c), and the resistance of the coating (R_c) are suitable to represent the material [23]. However, this condition remains valid for only a few minutes or seconds of immersion, depending on factors such as thickness, composition, and the dielectric constant of the coating [26][27]. When the electrolyte percolates, forming pores or channels and nano- or macro-structural defects, it is necessary to add a second time-constant to the EEC that represents an outer layer with the presence of pores (R_p and CPE_p) and a preserved inner layer of high impedance (R_c and CPE_c) [25][26]. Finally, the coating failure due to pitting determines the lifespan of the film. At this stage, a third time constant can be used to describe the behavior of the damaged material. The oxidation-reduction reactions taking place at the coating/metal interface can be described by charge transfer resistance (R_{ct}) in parallel with the capacitance of the electrical double layer (C_{DL}) [16][21][28].

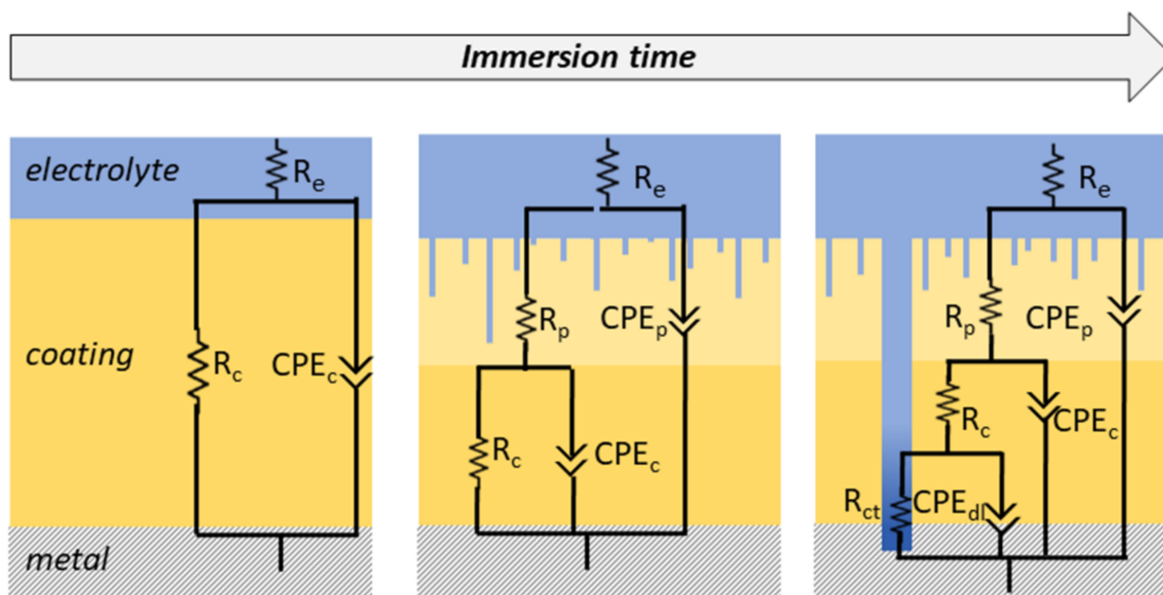


Figure 1. Representative schemes of electrical equivalent circuits (EECs) that are commonly used to fit EIS data of polymeric coatings over immersion time.

It is worthy to mention, however, that EIS tests by themselves do not represent a method for the unique and final analysis of protective coatings. To fully understand the system, the electrochemical measurements must be combined with structural, mechanical, and thermal investigations. For example, Fréchette et al. evaluated six different systems by combining accelerated corrosion tests in salt-spray chambers and Kesternich cabins with EIS tests, FTIR measurements, and adhesion tests [19]. They concluded that the joint analysis favored the understanding of the real-world conditions responsible for the degradation processes, providing valuable information about the best protective material for steel, namely epoxy and polyurethane coatings [19].

Relevant one in the field using the EIS technique have yielded significant discoveries. Among the main applications, studies of passive and active coatings also cover modeling to obtain physical parameters and water uptake calculations.

3. Advanced Electrochemical Analysis

The previous section was devoted to electrochemical measurements that represent an average of the electrochemical processes taking place on the entire surface of the working electrode. Below, it was described the main techniques

developed to detect the local corrosion reactions of active systems, which are documented with successful examples of their application for anti-corrosion polymeric coatings.

3.1. Localized Electrochemical Impedance Spectroscopy (LEIS)

The LEIS technique is based on the same principle as EIS. It measures the ratio between the applied AC voltage and the measured AC density between a sample and a counter electrode. Essentially, LEIS relies on the measurement of the local output current, which allows the calculation of the local impedance [29][30]. As a spatially resolved technique, the main applications of LEIS for polymeric coatings include tracking corrosion inhibition as well as the initiation and propagation of the delamination. While EIS provides only global surface-averaged responses, LEIS can provide highly accurate information on isolated defects (pits or scratches), which, in turn, corresponds to the global impedance due to the possibility of simultaneous measurements. LEIS is also a powerful technique to study substrate reactions underneath the coating. However, the size of the probe and the distance between the probe and substrate are important parameters that can affect the resolution of the results. It has been reported, for instance, that smaller probes provide better spatial resolutions [30].

The measurement of local impedance in the analysis of well-defined areas of polymeric coatings allows the obtaining of 2D or 3D color maps of defects and the observation of their regeneration when the film contains corrosion inhibitors/self-healing substances. Normally, LEIS maps are displayed in the admittance formalism, which is the inverse of the impedance ($Y = Z^{-1}$). In other words, for an active inhibition system, it is expected that a decrease in Y values will be observed over time.

Calado et al. investigated epoxy coatings modified with aminopropyltriethoxysilane (APTES) to improve the adhesion between the magnesium substrate AZ31 and CeO_2 , which is used to provide corrosion inhibition [31]. The LEIS tests were performed by submerging coatings with an artificial defect of about 750 μm in size in a 0.005 M NaCl solution, thus measuring blank and modified material after 0.5 h, 24 h, and 50 h of immersion. The evolution of the admittance values showed a different behavior for each coating. For the blank material, the admittance showed an increase of one order of magnitude after 50 h of immersion compared to the initial stages. However, the modified CeO_2 -coating delayed the onset of corrosion on the magnesium substrates by up to 35 h and showed much lower admittance variation [31]. The CeO_2 inhibitory activity in damaged coatings was thus confirmed by LEIS, with the admittance evolution over time compared to its initial value, reflected as a stable behavior in the presence of 325 ppm CeO_2 [31].

The self-healing action of cerium salts loaded within CaCO_3 microspheres was also confirmed in epoxy coatings on AA2024 substrates using LEIS [28]. With the addition of CaCO_3 as pH-sensitive containers, a decrease in admittance values over time (46 h) was observed in artificially damaged coatings immersed in a 1 mM NaCl solution. Combining LEIS (spatially resolved) and EIS results, the authors demonstrated the efficiency of inhibition provided by cerium salts in large-scale (6 mm \times 0.3 mm) defects [28]. The action of CeMo nanocontainers loaded on epoxy-silicate films was confirmed by LEIS elsewhere [32]. A 5 mM NaCl solution as an electrolyte was used during the measurement of artificially scratched films. The temporal evolution of admittance values showed that the reference coating exhibited an increase in corrosive activity, while the coating modified with the inhibitor showed a decrease in corrosion. The behavior observed by LEIS agrees with the EIS data, pointing to the reproducibility of the self-healing activity [32].

3.2. Scanning Vibrating Electrode Technique (SVET)

The use of a micro-tip (less than 20 μm) to detect the current distribution in solutions became an important tool for studying polymeric coatings and is based on the one carried out by Lilard et al. in 1992 [29]. The main outputs of SVET are ionic current density maps measured in the micrometer range of a corroding system that allow the visualization of the oxidation reactions at the anode sites and the reduction reactions at the cathode sites [23]. The measurements are performed in an electrochemical cell composed of a piezo-oscillator system that produces vibrations from the microelectrode that sweeps the coating surface (typically with artificial defects), a platinized reference electrode in the shape of a sphere (Pt/Ir: 80%/20%), and a signal amplifier [23]. After immersion in a conducting electrolyte, the current density distribution maps are generated as a result of DC potential gradients in the solution. SVET has been widely used to study active systems with corrosion inhibitors or self-healing agents; however, its application is limited to electrochemically active systems where DC currents flow in the solution so that corrosion reactions underneath intact coatings cannot be assessed [29]. Moreover, probe platinization and calibration can be laborious, not to mention its fragility and short lifespan. Nonetheless, SVET maps can be obtained in parallel with pH maps by coupling the scanning ion-selective electrode technique (SIET), thus making it a powerful tool to simultaneously analyze local current and pH changes [33].

With increasing interest in active and smart anti-corrosion systems, the number of publications reporting the use of SVET has grown significantly in recent years. For example, Lutz et al. presented SVET maps of a shape-recovery coating based on acrylated polycaprolactone polyurethane applied on hot-dip galvanized steel containing the corrosion inhibitor 2-Mercaptobenzothiazole (MBT) loaded in layered double hydroxide (MLDH) [34]. The system containing the MLDH was compared with the reference material. As shown in **Figure 2**, the release of MBT at the active corrosion sites resulted in a significant decrease in current densities (from $\pm 12 \mu\text{A}/\text{cm}^2$ to $\pm 2\text{--}3 \mu\text{A}/\text{cm}^2$). The ionic current density maps were recorded after 4 h of immersion at 100 μm from the surface [34].

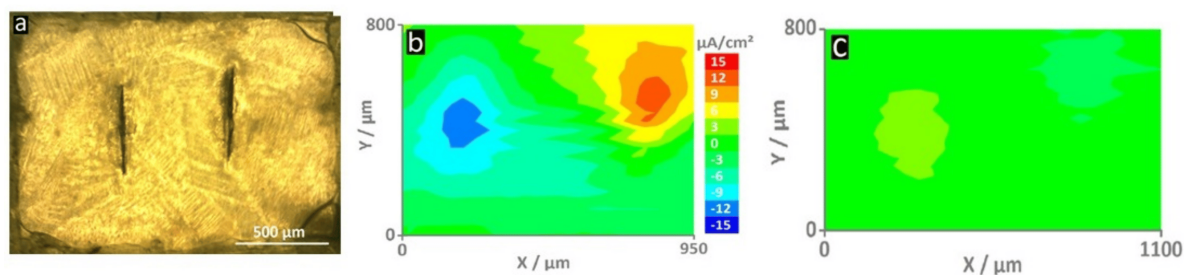


Figure 2. Optical micrographs of (a) the self-healing surface with two vertical screwdriver-blade indentations that form the defects through the coating. The map of the reference sample shows (b) high current densities ($\pm 12 \mu\text{A}/\text{cm}^2$) - an indication of an actively corroding sample. On the contrary, the sample with MLDH (c) shows much smaller current densities and thus corrosion inhibition [34].

The results provided by SVET improve the understanding of the inhibition mechanisms of corrosion inhibitors. The activity of inorganic compounds such as cerium salts in epoxy–silane hybrids on magnesium alloy AZ31 [35] or organic agents such as 8-hydroxyquinoline (8HQ) in sol-gel films prepared from zirconium (IV) propoxide on AA2024 [36] was unveiled with the use of SVET. In the case of cerium salts, the Ce^{3+} cations react with the OH^- anions released in the cathodic zone to form $\text{Ce}(\text{OH})_3$, a very stable compound at 25 $^\circ\text{C}$ ($K_{\text{sp}} \text{Ce}(\text{OH})_3 = 6.3 \times 10^{-24}$), which inhibits cathodic activity and, consequently, the corrosion processes [37]. On the other hand, the action of 8HQ is based on the formation of chelate complexes with copper or aluminum, suppressing the initial stages of localized corrosion attacks [36].

3.3. Scanning Ion-Selective Electrode Technique (SIET)

The setup of SIET measurements is similar to that of SVET measurements. However, in this technique, an ion-selective microelectrode, in the form of a glass capillary, is used to scan the surface in a 3D computerized system. The microelectrode is filled with a liquid membrane capable of measuring ions down to the picomolar level, the electrolyte, and an Ag/AgCl wire as a reference electrode [38]. This membrane is composed of different ionic species that can be chosen, for example, according to the pH range to be studied. SIET is a powerful technique for the evaluation of corrosion inhibitors' efficiency by identifying the pH gradients in active systems with good lateral resolution. Although the possibility of filling glass capillaries with different membranes is an advantage, working with microelectrodes is not an easy task because they are brittle and their lifetime is limited to a few hours or a maximum of one day [38]. In addition, silanization of the capillary is required to hold the membrane. When this step is not properly performed, the membrane leaks easily, making the operation time-consuming and difficult.

Knowledge of the local surface pH can help identify the mechanisms of corrosion inhibitors in specific regions, considering the local pH variations that occur in the anodic and cathodic regions. It is also of great importance to choose corrosion inhibitors appropriately according to the working pH range and substrate [39]. Visser et al. observed significant pH variations into scratched areas of polyurethane coatings on AA2024 by incorporating different lithium salts (carbonate and oxalate) [40].

Others with cerium-based corrosion inhibitors reported interesting results for the SIET measurements. For example, the addition of CeO_2 [31] or cerium phosphate [35] to epoxy–silane coatings on an AZ31 magnesium alloy provided indications of a local pH shift induced by the reaction between Ce and hydroxyl ions in the cathodic regions [31][35]. In addition to investigations of the self-healing effect, SIET maps are useful for comparative ones of metallic alloys, such as the analysis of corrosion mechanisms for different magnesium alloys, such as AZ31 and ZE41 [41]. The higher corrosive activity of AZ31 observed by SIET and SVET was reflected in the more pronounced differences in pH and current density values (80 $\mu\text{A cm}^{-2}$ for ZE41 vs. 120 $\mu\text{A cm}^{-2}$ for AZ31) [41].

3.4. Scanning Kelvin Probe (SKP)

A variant of atomic force microscopy (AFM), scanning Kelvin probe (SKP), can be obtained by applying the non-contact scan mode to generate surface topography maps and potential distribution of the work function (or Volta potential). A decrease in the Volta potential can be considered as an increased tendency for electrochemical reactions [42]. SKP is widely used in coatings and corrosion ones, but it can also be applied to measurements of the composition and electronic state of a solid's local structure. These other solids include catalysts, semiconductor doping, dielectric materials, investigation of intermetallic in alloys, and others [42]. Its major advantages include measuring the electrode potential without touching the surface, since the reference electrode is connected to the sample through a metallic wire and separated by a dielectric medium (for instance, under a vacuum). SKP, also known as Kelvin probe force microscopy (KPFM), is a versatile tool for the analysis of polymeric coatings and can be operated in open-air, humid air, or by using a single drop of electrolyte. Although it provides limited spatial resolution (about 100 μm for a 150 μm probe diameter), resolutions in the nanometer range can be achieved when it is coupled with an AFM [33].

SKP is widely applied in conducting polymeric coatings (CPCs). The combination of electronic properties of semiconductors and the processing of conventional polymers makes this type of material an interesting alternative for anti-corrosion applications [43]. Various mechanisms have been proposed to explain their anti-corrosion properties, such as controlled inhibitor release, barrier properties, and anodic protection [44]. In particular, the latter mechanism is known due to observations of the oxygen-reduction reactions shifting from the coating/substrate interface to the coating/electrolyte interface, thus preventing the delamination of the coating [44]. On that basis, SKP is a useful tool to investigate the delamination kinetics of CPCs. By using SKP, for example, it was shown that small cations from the electrolyte can permeate polypyrrole-based films, causing faster delamination of the coating [44].

Bai et al. observed a significant reduction in the delamination rate by adding carbon black (CB) to poly (3,4-ethylene dioxythiophene) nanoparticles (PEDOT) and polyvinyl butyral (PVB) coatings on zinc substrates [45]. The PEDOT/CB/PVB composites slowed the cathodic delamination to 10 $\mu\text{m h}^{-1}$ and even stopped after 3 days of immersion in 1 M KCl [45]. Yin and co-authors on polypyrrole coatings modified with organic corrosion inhibitors such as β -Cyclodextrine (β -CD), benzotriazole (BTA), or 8-Hydroxyquinoline (8-HQ) used SKP to evaluate their self-healing performance [46]. Excellent passivation was observed by monitoring the corrosion potential and SKP profiles for the artificially damaged polypyrrole–BTA coating. This performance is proposed to be a consequence of the anodic polarization by the re-oxidizing polypyrrole and the BTA activity that fully restored the delaminated interface [46]. In a similar one, the mobility of different corrosion inhibitors through the partially reduced polypyrrole coating was compared, and they found higher activity for cationic inhibitors due to the cation-permselectivity of this polymeric matrix [47]. Electrochemical passivation through re-oxidation of polypyrrole was also observed, resulting in potential shifts of up to 700 mV, an effect potentiated by the combination of conductive polymers and corrosion inhibitors [47].

3.5. Scanning Electrochemical Microscopy (SECM)

SECM combines high electrochemical sensitivity with spatial resolution, resulting in a powerful tool for characterizing a variety of electrochemical reactions in active coating systems. The principle of operation of SECM is simple: a microelectrode (Pt wire) scans the surface of a sample immersed in an electrolyte, providing information on the topography and/or redox reactions taking place at the interface tip/sample [23]. One of the main advantages of SECM is its simultaneous characterization of the topography and redox activity of immersed samples. In other words, it is possible to obtain information about the reactions that take place on the surface and in the space between the tip and the sample [23]. Its usefulness can be attributed to its high lateral resolution when compared to SVET due to the wide range of electrode sizes, allied with the possibility of combining it with other techniques in several modes of operation. As the main drawbacks of SECM, one can mention the need for a bipotentiostat to polarize the microelectrode and sample, the dependence of the resolution on the microelectrode size and distance from the surface, and competing redox reactions that can occur at the probe and surface at the same time [23][33].

SECM was used to study the addition of decavanadate-intercalated layered double hydroxide (LDH-VS) loaded into sol-gel films on AA2024 aluminum alloy. The results of artificially scratched samples show the absence of lateral delamination towards the film side, probably caused by the structural and adhesion improvement provided by LDH-VS [48]. In another report, the recovery of the barrier properties of shape-memory epoxy coatings (50 \pm 5 μm thickness) modified with carnauba wax microparticles was also observed by SECM [49].

References

1. Meade, C.L. Accelerated corrosion testing. *Met. Finish.* 1999, 97, 526–531.
2. Holden, H. How carefully do you control your salt spray test? *Anti-Corros. Methods Mater.* 1955, 2, 157–163.
3. Bierwagen, G.P.; He, L.; Li, J.; Ellingson, L.; Tallman, D. Studies of a new accelerated evaluation method for coating corrosion resistance—Thermal cycling testing. *Prog. Org. Coat.* 2000, 39, 67–78.
4. Blakey, R. Evaluation of paint durability-natural and accelerated. *Prog. Org. Coat.* 1985, 13, 279–296.
5. ASTM B117-16; Standard Practice for Operating Salt Spray (Fog) Apparatus. ASTM International: West Conohohocken, PA, USA, 2016.
6. Lazzari, L. Testing. In *Engineering Tools for Corrosion*; Lazzari, L., Ed.; Woodhead Publishing: Cambridge, UK, 2017; pp. 119–129. ISBN 9780081024249.
7. Visser, P.; Liu, Y.; Terryn, H.; Mol, J.M.C. Lithium salts as leachable corrosion inhibitors and potential replacement for hexavalent chromium in organic coatings for the protection of aluminum alloys. *J. Coat. Technol. Res.* 2016, 13, 557–566.
8. Thuy, D.N.; Xuan, H.T.T.; Nicolay, A.; Paint, Y.; Olivier, M.-G. Corrosion protection of carbon steel by solvent free epoxy coating containing hydrotalcites intercalated with different organic corrosion inhibitors. *Prog. Org. Coat.* 2016, 101, 331–341.
9. Castro, Y.; Özmen, E.; Durán, A. Integrated self-healing coating system for outstanding corrosion protection of AA2024. *Surf. Coat. Technol.* 2020, 387, 125521.
10. Zheludkevich, M.; Poznyak, S.; Rodrigues, L.; Raps, D.; Hack, T.; Dick, L.F.P.; Nunes, T.; Ferreira, M.G.S. Active protection coatings with layered double hydroxide nanocontainers of corrosion inhibitor. *Corros. Sci.* 2010, 52, 602–611.
11. Díaz, I.; Chico, B.; De la Fuente, D.; Simancas, J.; Vega, J.; Morcillo, M. Corrosion resistance of new epoxy–siloxane hybrid coatings. A laboratory study. *Prog. Org. Coat.* 2010, 69, 278–286.
12. Xia, D.-H.; Deng, C.-M.; Macdonald, D.; Jamali, S.; Mills, D.; Luo, J.-L.; Strebl, M.G.; Amiri, M.; Jin, W.; Song, S.; et al. Electrochemical measurements used for assessment of corrosion and protection of metallic materials in the field: A critical review. *J. Mater. Sci. Technol.* 2022, 112, 151–183.
13. Fandi, M.; Liu, L. Electrochemical Evaluation Technologies of Organic Coatings. In *Coatings and Thin-Film Technologies*; Jaime, A.P.-T., Bernal, A.G.A., Eds.; IntechOpen: London, UK, 2018; pp. 49–67. ISBN 978-1-78984-871-7.
14. Wolstenholme, J. Electrochemical methods of assessing the corrosion of painted metals—A review. *Corros. Sci.* 1973, 13, 521–530.
15. Pourbaix, M. Applications of electrochemistry in corrosion science and in practice. *Corros. Sci.* 1974, 14, 25–82.
16. Trentin, A.; Harb, S.V.; Uvida, M.C.; Pulcinelli, S.H.; Santilli, C.V.; Marcoen, K.; Pletincx, S.; Terryn, H.; Hauffman, T.; Hammer, P. Dual Role of Lithium on the Structure and Self-Healing Ability of PMMA-Silica Coatings on AA7075 Alloy. *ACS Appl. Mater. Interfaces* 2019, 11, 40629–40641.
17. Boumezgane, O.; Suriano, R.; Fedel, M.; Tonelli, C.; Deflorian, F.; Turri, S. Self-healing epoxy coatings with microencapsulated ionic PDMS oligomers for corrosion protection based on supramolecular acid-base interactions. *Prog. Org. Coat.* 2022, 162, 106558.
18. Ohtsuka, T. Corrosion Protection of Steels by Conducting Polymer Coating. *Int. J. Corros.* 2012, 2012, 915090.
19. Fréchette, E.; Compere, C.; Ghali, E. Evaluation of the corrosion resistance of painted steels by impedance measurements. *Corros. Sci.* 1992, 33, 1067–1081.
20. Loveday, D.; Peterson, P.; Rodgers, B. Evaluation of Organic Coatings with Electrochemical Impedance Spectroscopy. Part 2: Application of EIS to Coatings. *J. Coat. Technol.* 2004, 1, 88–93.
21. Bonora, P.; Deflorian, F.; Fedrizzi, L. Electrochemical impedance spectroscopy as a tool for investigating underpaint corrosion. *Electrochim. Acta* 1996, 41, 1073–1082.
22. Razin, A.A.; Ramezanzadeh, B.; Yari, H. Detecting and estimating the extent of automotive coating delamination and damage indexes after stone chipping using electrochemical impedance spectroscopy. *Prog. Org. Coat.* 2016, 92, 95–109.
23. Gonzalez-Garcia, Y.; Espallargas, S.G.; Mol, J.M.C. Electrochemical Techniques for the Study of Self Healing Coatings. In *Active Protective Coatings: New-Generation Coatings for Metals*; Hughes, A.E., Mol, J.M.C., Zheludkevich, M.L., Buchheit, R.G., Eds.; Springer: Dordrecht, The Netherlands, 2016; pp. 203–240. ISBN 9783642275111.

24. House, L.H. Instruments and Corrosion. *Corros. Technol.* 1960, 7, 222–223.
25. Trentin, A.; Gasparini, A.D.L.; Faria, F.A.; Harb, S.V.; Dos Santos, F.C.; Pulcinelli, S.H.; Santilli, C.V.; Hammer, P. Barrier properties of high performance PMMA-silica anticorrosion coatings. *Prog. Org. Coat.* 2020, 138, 105398.
26. Bouvet, G.; Nguyen, D.D.; Mallarino, S.; Touzain, S. Analysis of the non-ideal capacitive behaviour for high impedance organic coatings. *Prog. Org. Coat.* 2014, 77, 2045–2053.
27. Nguyen, A.S.; Musiani, M.; Orazem, M.E.; Pébère, N.; Tribollet, B.; Vivier, V. Impedance analysis of the distributed resistivity of coatings in dry and wet conditions. *Electrochim. Acta* 2015, 179, 452–459.
28. Snihirova, D.; Lamaka, S.; Montemor, F. “SMART” protective ability of water based epoxy coatings loaded with CaCO₃ microbeads impregnated with corrosion inhibitors applied on AA2024 substrates. *Electrochim. Acta* 2012, 83, 439–447.
29. Lillard, R.S.; Moran, P.J.; Isaacs, H.S. A Novel Method for Generating Quantitative Local Electrochemical Impedance Spectroscopy. *J. Electrochem. Soc.* 1992, 139, 1007–1012.
30. Huang, V.M.; Wu, S.-L.; Orazem, M.E.; Pébère, N.; Tribollet, B.; Vivier, V. Local electrochemical impedance spectroscopy: A review and some recent developments. *Electrochim. Acta* 2011, 56, 8048–8057.
31. Calado, L.M.; Taryba, M.G.; Carmezim, M.J.; Montemor, M.F. Self-healing ceria-modified coating for corrosion protection of AZ31 magnesium alloy. *Corros. Sci.* 2018, 142, 12–21.
32. Kartsonakis, I.; Athanasopoulou, E.; Snihirova, D.; Martins, B.; Koklioti, M.; Montemor, M.; Kordas, G.; Charitidis, C. Multifunctional epoxy coatings combining a mixture of traps and inhibitor loaded nanocontainers for corrosion protection of AA2024-T3. *Corros. Sci.* 2014, 85, 147–159.
33. Jadhav, N.; Gelling, V.J. Review—The Use of Localized Electrochemical Techniques for Corrosion Studies. *J. Electrochem. Soc.* 2019, 166, C3461–C3476.
34. Lutz, A.; Van den Berg, O.; Wielant, J.; De Graeve, I.; Terryn, H. A Multiple-Action Self-Healing Coating. *Front. Mater.* 2016, 2, 73.
35. Calado, L.M.; Taryba, M.G.; Morozov, Y.; Carmezim, M.; Montemor, M.F. Novel smart and self-healing cerium phosphate-based corrosion inhibitor for AZ31 magnesium alloy. *Corros. Sci.* 2020, 170, 108648.
36. Yasakau, K.; Carneiro, J.; Zheludkevich, M.; Ferreira, M. Influence of sol-gel process parameters on the protection properties of sol-gel coatings applied on AA2024. *Surf. Coat. Technol.* 2014, 246, 6–16.
37. Varshney, S.; Chugh, K.; Mhaske, S.T. Effect of layer-by-layer synthesized graphene–polyaniline-based nanocontainers for corrosion protection of mild steel. *J. Mater. Sci.* 2022, 57, 8348–8366.
38. Lamaka, S.V.; Souto, R.M.; Ferreira, M.G.S. In-Situ Visualization of Local Corrosion by Scanning Ion-Selective Electrode Technique (SIET). In *Microscopy: Science, Technology, Applications and Education*; Formatex Research Center: Badajoz, Spain, 2010; Volume 3, pp. 2162–2173.
39. Yasakau, K.A.; Zheludkevich, M.L.; Lamaka, S.V.; Ferreira, M.G.S. Mechanism of Corrosion Inhibition of AA2024 by Rare-Earth Compounds. *J. Phys. Chem. B* 2006, 110, 5515–5528.
40. Visser, P.; Lutz, A.; Mol, J.; Terryn, H. Study of the formation of a protective layer in a defect from lithium-leaching organic coatings. *Prog. Org. Coat.* 2016, 99, 80–90.
41. Córdoba, L.C.; Marques, A.; Taryba, M.; Coradin, T.; Montemor, F. Hybrid coatings with collagen and chitosan for improved bioactivity of Mg alloys. *Surf. Coat. Technol.* 2018, 341, 103–113.
42. Örnek, C.; Leygraf, C.; Pan, J. On the Volta potential measured by SKPFM—fundamental and practical aspects with relevance to corrosion science. *Corros. Eng. Sci. Technol.* 2019, 54, 185–198.
43. Rohwerder, M. Conducting polymers for corrosion protection: A review. *Int. J. Mater. Res.* 2009, 10, 1331–1342.
44. Deshpande, P.P.; Jadhav, N.G.; Gelling, V.J.; Sazou, D. Conducting polymers for corrosion protection: A review. *J. Coat. Technol. Res.* 2014, 11, 473–494.
45. Bai, X.; Tran, T.H.; Yu, D.; Vimalanandan, A.; Hu, X.; Rohwerder, M. Novel conducting polymer based composite coatings for corrosion protection of zinc. *Corros. Sci.* 2015, 95, 110–116.
46. Yin, Y.; Prabhakar, M.; Ebbinghaus, P.; Da Silva, C.C.; Rohwerder, M. Neutral inhibitor molecules entrapped into polypyrrole network for corrosion protection. *Chem. Eng. J.* 2022, 440, 135739.
47. Yin, Y.; Schulz, M.; Rohwerder, M. Optimizing smart self-healing coatings: Investigating the transport of active agents from the coating towards the defect. *Corros. Sci.* 2021, 190, 109661.
48. Wu, J.; Peng, D.; Junsheng, W.; Du, X.; Zhang, Z.; Zhang, B.; Li, X.; Huang, Y. In Situ Formation of Decavanadate-Intercalated Layered Double Hydroxide Films on AA2024 and their Anti-Corrosive Properties when Combined with Hybrid Sol Gel Films. *Materials* 2017, 10, 426.

49. Wang, L.; Deng, L.; Zhang, D.; Qian, H.; Du, C.; Li, X.; Mol, A.; Terryn, H. Shape memory composite (SMC) self-healing coatings for corrosion protection. *Prog. Org. Coat.* 2016, 97, 261–268.
-

Retrieved from <https://encyclopedia.pub/entry/history/show/58637>